



## The Effect of Laser Power on Tensile Strength and Microstructure of Ti-6Al-4V ELI Fabricated By Selective Laser Melting

Pajaree Termrungruanglert<sup>1,\*</sup>, Viritpon Srimaneepong<sup>1</sup> and Prasit Pavasant<sup>2</sup>

<sup>1</sup>Department of Prosthodontics, Faculty of Dentistry, Chulalongkorn University, Bangkok, Thailand

<sup>2</sup>Department of Anatomy, Faculty of Dentistry, Chulalongkorn University, Bangkok, Thailand

\*Corresponding author, E-mail: pajaree.term@gmail.com

### Abstract

Titanium is commonly used in biomedical applications because it is dominant in many properties such as good biocompatibility, high corrosive resistance, high specific strength, and nonmagnetic property. At present, fabricating titanium devices or orthopedic parts by selective laser melting (SLM) has gained interest due to its advantages over conventional methods such as casting, or milling. Laser power is one of the factors that affect the mechanical properties during the SLM process. This study aimed to examine the effect of the various laser powers on the tensile strength and microstructure of Ti-6Al-4V ELI. The Ti-6Al-4V ELI alloy samples were printed in dumbbell shape by SLM machine (Trumpf/TruPrint 1000, Germany) with 3 laser powers (75, 100, and 125 W), 6 samples for each group. All samples were performed under a tensile test with a universal testing machine, and data were analyzed with one-way ANOVA and Tukey's post hoc tests ( $\alpha=0.05$ ). The microstructure was analyzed by optical microscope and the mode of failure was observed by SEM. The results showed that the laser power of 100 W with a spot size of 30  $\mu\text{m}$ , scanning speed of 600 mm/s, and layer thickness of 30  $\mu\text{m}$  (fixed parameters) was suitable to achieve the highest tensile strength, compared with the other 2 groups. The mode of failure after tensile testing in the 75 and 100 W laser power groups showed both ductile and brittle fractures. The 125 W laser power group is a predominantly brittle fracture.

**Keywords:** 3D-printing, selective laser melting, SLM, titanium grade 23, tensile strength

### 1. Introduction

Titanium and its alloy are being used increasingly for a variety of applications. Examples include aircraft, aero-engines, components in chemical processing equipment, and also in the biomedical field (Wysocki et al., 2017). The most common application of titanium is an implant in the biomedical field because it is dominant in many properties such as good biocompatibility, high corrosive resistance, high specific strength, nonmagnetic property, and low specific gravity (Frazier, 2014).

Titanium grade 5, also known as Ti-6Al-4V (Ti64) alloy. It consists of 90% titanium, 6% aluminum, and 4% vanadium. Besides, It is a biphasic microstructure, which is an  $\alpha + \beta$  titanium alloy (Trevisan et al., 2017). Aluminum stabilizes the alpha phase that helps in corrosion resistance but is low in tensile strength. Vanadium stabilizes the beta phase that helps in ductility and resistance in plastic deformation (Trevisan et al., 2017). Ti-6Al-4V ELI or Titanium grade 23 is fundamentally a grade 5 titanium but the weight of oxygen (O), iron (Fe), and nitrogen (N) are less for low interstitial alloy. It improves ductility and fracture toughness with some reduction in strength. It is used as surgical implant in the medical field such as plates and screws due to the biocompatibility. In the aircraft field, it is used in gas turbine engines, including all parts of the aircraft (Singh et al., 2020).

In the past, titanium could be manufactured by casting and wrought but today Additive Manufacturing or AM has become widespread because of the advantages over traditional methods, for example, reducing material consumption and fabricates complex applications (Ahmad & Al-Harbi, 2018; Schulze, Weinmann, Schweigel, Kessler, & Bader, 2018; Trevisan et al., 2017). AM or 3D printing is a procedure of joining material to make objects from 3D model data, usually layer by layer. Selective laser melting (SLM) is one of the 3D printing technology. SLM is usually used for producing metal powder works. The first step is designing a 3D model by using computer-aided design (CAD) software. The 3D CAD file is



a STereoLithography(.stl) file format. Subsequently, the STL files are forwarded to an SLM machine for realizing and printing the final product. The main parameters are laser power, scan speed, layer thickness, and scan spacing or hatch space. These factors must be controlled to achieve the quality of the workpiece because these parameters affect the laser energy density (J). In general, the primary goals for SLM are the full density and free of defect. During the SLM processing, power of laser beam interacts to the powder bed with the constant scan speed. Layer thickness is a layer of powder. Moreover, scan spacing or hatch space is defined as the overlap of adjacent solidified metal; therefore, it significantly affects the porosities and surface roughness (Sing, 2019b).

The correlation of these manufacturing parameters is explained in the equation below (El-Sayed, Ghazy, Youssef, & Essa, 2018; Zhang & Attar, 2016).

$$\text{Laser energy density} = \frac{\text{laser power}}{\text{scan speed} \times \text{layer thickness} \times \text{scan spacing}}$$

The first parameter is laser power, which affects the recoil pressure, wettability, surface tension, and the depths of heat penetration of the molten pool (Elsayed, 2019; Kusuma, Ahmed, Mian, & Srinivasan, 2017). Thus, the surface of SLM improves the physical property due to less porosity and reduced roughness in both the top and side surfaces. The mechanical properties such as tensile strength and Young's modulus would be improved (Elsayed, 2019; Liu et al., 2019). Scanning speed affects the melting pool directly. The optimal scanning speed can make the regular melting pool with no defect. While the high scanning speed makes the irregular melting pool with multiple boundaries in SEM (Liu et al., 2019). Using very high scanning speeds may decrease the bonding between the deposited layers and consequently reducing the mechanical properties (Azarniya et al., 2019). Layer thickness is an inverse factor to the laser energy density. The layer thickness can affect the connecting between melted metal powder. The higher layer thickness will increase nodulizing and incomplete layer workpiece, resulting in porosity (J. Sun, Yang, & Wang, 2013). The last parameter is scan spacing or hatching space, which is the length between the two laser scans. It least impact the process parameters (Shipley et al., 2018). The less hatching space increases the overlapping area besides scanning lines. Subsequently, the uniform distribution of energy will make the metal powder melt completely. However, the overburning of the meting pool can be caused by too small scan spacing (J. Sun et al., 2013). The laser energy density affects the microstructure formation during the solidification and finally determines the resultant properties of the SLM metal (Wang & Li, 2018). A mixture of alpha phase, beta phase, and acicular martensitic  $\alpha'$  phase has been observed in the microstructure SLM Ti-6Al-4V alloy. The presence of acicular martensites in the SLM Ti-6Al-4V alloy leads to a significant improvement in tensile strength from 900 to 1450 MPa but considerably reduced ductility (Song, Dong, Zhang, Liao, & Coddet, 2012).

The SLM has many advantages over conventional production methods such as manufacturing complex geometries and reducing human resources and waste material. Today, there are many SLM titanium alloy used in clinical applications in both medical and dental fields. For example, in the orthopaedic field, the practitioners create a 3D model in CAD for customized hip and printed in titanium implant for Total Hip Replacement (THR). In the dentistry field, the removable partial denture can fabricated by designing in CAD and printed in CoCr framework (Alifui-Segbaya, Williams, & George, 2017). Many research studied the effect of the laser parameters on mechanical properties. However, the relationship between the laser power and the mechanical properties of Ti-6Al-4V ELI has not been completely understood, and more systematic research work is necessary to attain a better understanding of these features. In this study, the samples were fabricated with different laser powers while several studies investigated the results by varying other factors. Most of them usually varied multi factors and used the statistic for calculating. Thus, this study aimed to vary only the laser power and keep others parameters constant, including scan speed, layer thickness, and scan spacing that were fixed. The optimum values for these parameters (spot size, scan speed, layer thickness, and scan spacing) were defined by an internal algorithm of the 3D metal printer (Trumpf/TruPrint 1000, Germany). In this research, the researchers used tensile testing to study the effect of the laser power because Ti-6Al-4V ELI is metal alloy and biomaterial implant. It must follow the standard specification of ASTM



F136-13(ASM, 2013) that determines the mechanical properties in tensile strength.

## 2. Objectives

1. To examine the effect of different laser powers on tensile strength of Ti-6Al-4V ELI alloy
2. To examine the effect of different laser powers on microstructure of Ti-6Al-4V ELI alloy

## 3. Materials and Methods

### 3.1 Powder materials and SLM process

Ti-6Al-4V ELI alloy (Ti Grade 23) (AP&C, USA) chemical compositions of the materials were presented in Table 1. The powder had a spherical shape. The samples were fabricated by varying the laser powers into 3 groups (75, 100, 125 W), 6 samples for each group. The other manufacturing parameters were defined by an internal algorithm (spot size 30  $\mu\text{m}$ , scanning speed 600 mm/s, and layer thickness 30  $\mu\text{m}$ ) of the 3D metal printer (Trumpf/TruPrint 1000, Germany).

**Table 1** Chemical composition of Ti-6Al-4V ELI

Composition	Al	V	Fe	O	C	N	H
wt%	3.5-6.5	3.5-4.5	<0.25	<0.25	<0.08	<0.05	<0.012

The powder of Ti-6Al-4V ELI was printed in a dumbbell shape with a diameter of 9 mm (D) and gauge length of 26 mm (G) in accordance with ASTM E 8M-04 (ASTM, 2004) and followed the size of grip in the universal testing machine.

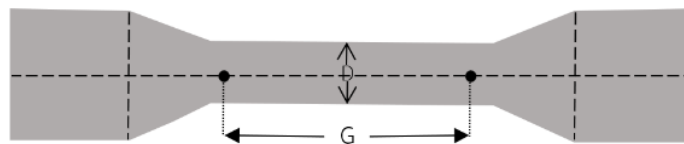


**Figure 1** The geometry and dimension of the sample

### 3.2 Tensile test

Uniaxial tensile test was performed using the universal testing machine (SHIMADZU 100kN, Japan). The tensile test was performed at room temperature and equipped with a 1.0 kN load cell enabling the force measurement with a precision of 0.1 N. The tensile test specimens were deformed to failure at a fixed crosshead speed of 0.3 mm/min. The test was performed until the sample was broken.

### 3.3 Observation of microstructure and mode of failure

After fractured from the tensile test, the specimens were visually analyzed under a scanning electron microscope (SEM) (FEI Quanta 250, USA) at x100 and x300 magnification to analyze modes of failure. Failure modes were classified into three types. There are ductile fractures, brittle fractures, and combined fractures with ductile and brittle fractures. The ductile fractures were dimple or honeycomb-like characteristics, whereas the brittle fractures were well-defined crystallographic plane or cleavage step.

Then the samples from all groups were randomly prepared for microstructure analysis. And the samples were embedded in Bakelite molding in diameter 1 inch. The mounted specimens were polished using a polishing machine (Nano 2000, Pace technologies, USA) up to 2000 SiC paper and etched with Kroll's reagent (100 mL H<sub>2</sub>O, 5 mL HNO<sub>3</sub>, and 2.5 mL HF) for 20 seconds. The microstructure of the specimens was observed by stereomicroscope (BX51M, Olympus, Japan) at x500 magnification.

### 3.4 Statistical analysis

Shapiro-Wilk and Levene's tests were performed for checking normality and homogeneity of variances, respectively by SPSS (statistical analysis software version 22.0, Chicago, IL, USA). One-way ANOVA and Tukey's posthoc analysis was used to analyze tensile strength. The significance level was set at  $\alpha = 0.05$ .



#### 4. Results and Discussion

##### 4.1 Results

##### 4.1.1 Tensile test

**Table 2** Tensile strength

Laser power (Watt)	N	Mean and SD Tensile strength (MPa)
75	6	452.00±96.90 <sup>A</sup>
100	6	1189.39±21.53 <sup>B</sup>
125	6	317.50±103.02 <sup>C</sup>

Different capital superscript letters indicate that tensile strength values were significantly different at  $p < 0.05$

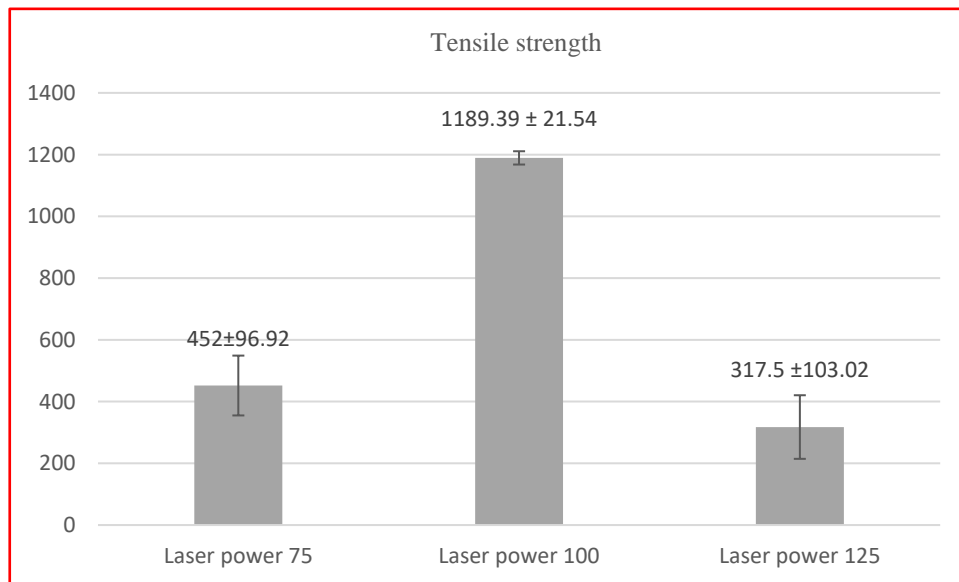
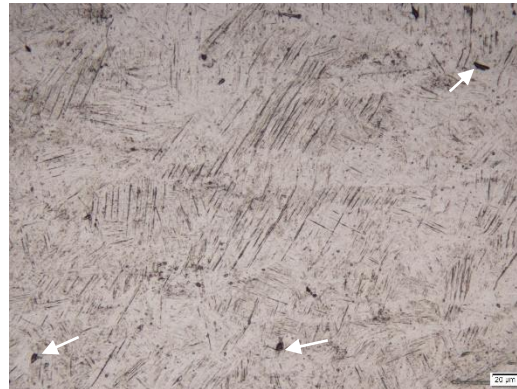


**Figure 2** Tensile strength (MPa). Value presented by means  $\pm$  SD

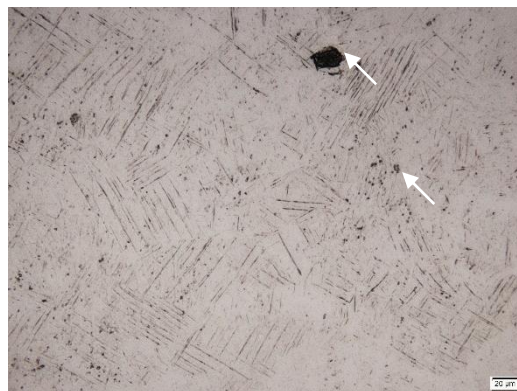
#### 4.1.2 Microstructure analysis



(a)



(b)



(c)

**Figure 3** Light optical microscope images of 3 different SLM Ti-6Al-4V ELI groups at x500 magnification (a) 75W, (b) 100 W, and (c) 125 W. The white arrows indicate the porosity. The dark arrows indicate the presence of  $\alpha'$  martensitic phase.

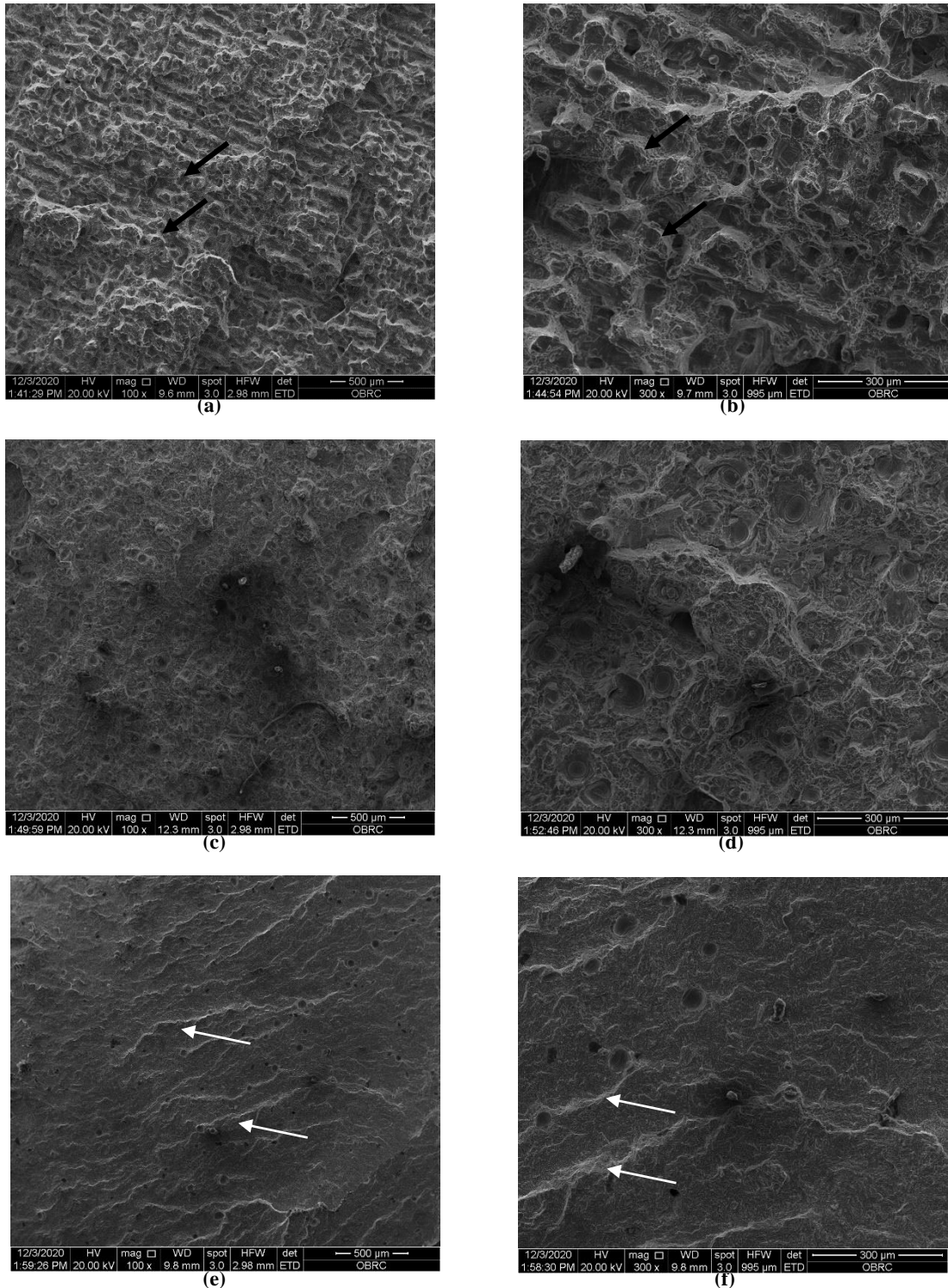


**Figure 4** Fractographic images of 3 different SLM Ti-6Al-4V ELI groups. (a,b) 75 W, (c,d) 100 W, and (e,f) 125 W at x100 and x300 magnification, respectively. The dark arrows indicate the presence of the dimple fracture. The white arrows indicate the presence of the transgranular cleavage facet.



#### 4.2 Discussion

From optical microscope, the researchers found some porosity in the 75 and 125 W laser power groups (Figures 3a and 3c) dispersing through the specimen. The porosity caused the lower tensile strength (Attar, Calin, Zhang, Scudino, & Eckert, 2014). The researchers suppose that the lower laser power (low laser energy density) in the 75 W laser power group could make an incomplete melting pool during the SLM process, causing defects and irregularity in the samples (Attar et al., 2014). However, the over-concentrated laser energy in the 125 W laser power group would bring overburning that may influence the density of the samples (J. Sun et al., 2013), leading to low tensile strength. However, as mentioned above, the laser energy density does not depend solely on laser power, but other parameters such as scan speed, layer thickness, and scan spacing can affect the microstructure and mechanical properties as well.

Thus, the laser power of 100 W is the level of proper properties since this group had high tensile strength and low porosity. The researchers found that the laser power of 100 W and other parameters (spot size 30  $\mu\text{m}$ , scanning speed 600 mm/s, and layer thickness 30  $\mu\text{m}$ ) could produce nearly fully dense density by melting the metal powder completely (Dong et al., 2020). The less defect and refined  $\alpha'$  martensitic microstructure as indicated by the dark arrow in Figure 3b produced more density of melted metal and led to better mechanical property.

This study corresponds to a study by Choo et al in 2019 on stainless steel and claimed that varying the laser powers from 200 to 380 W with a constant scan speed of 300 mm/s resulted in decreased the porosity from 0.88 to 0.13 % (Choo et al., 2019). Furthermore, another study by Attar et al. on commercially pure titanium that varied the laser powers between 70 to 250 W with a scan speed of 20-180 mm/s found that the laser power of 165 W and a scan speed of 138 mm/s provided the highest density of titanium. However, they also claimed that the laser power of higher than 180 W did not improve the density of titanium. SEM fractography showed that the type of failure mode was a mixed failure mode in the 75 and 100 W laser power groups (Figures 4a, b, c, and d). However, the 75 W laser power group (Figures 4a and b) extinguished many dimples characteristic when compared with the 100 W laser power group (Figures 4c and d). The dimples or honeycomb-like characteristic remarks in ductile fractures but the 125 W laser power group mostly showed the characteristic of brittle fractures, which was transgranular cleavage facet (Figures 4e and f). Besides, the cracks of tensile failure initiated and extended around the porosity or defects (Gong, 2013).

Corresponding to the study by Sun et al. in 2018, they found that the fracture surface of the SLM Ti-6Al-4V samples exhibited both brittle and ductile fractures in high laser energy densities but caused unmelted metal powder in low laser energy densities, thus the fractography presented more dimples of ductile failures (Sun et al., 2019).

This study may provide better knowledge about the effect of laser power on SLM Ti-6Al-4V ELI in mechanical properties and the microstructure and may improve the mechanical properties of medical and dental implants in the future.

The limitation is that our studies did not investigate the effect of the scan strategy or building orientation during the printing process. There are many patterns such as stripes, chessboards, and meanders (Sing, 2019a). Recently, some research has studied this effect on the physical and mechanical properties. Further research could study the effect of post treatment of SLM Ti-6Al-4V ELI alloy on mechanical properties. Moreover, the biological studied in SLM Ti-6Al-4V ELI alloy could be investigated.

#### 5. Conclusion

By varying the laser power while keeping other laser parameters constant, SLM Ti-6Al-4V ELI prepared by the laser power of 100 W showed the highest tensile strength with the  $\alpha'$  martensitic phase microstructure.

#### 6. Acknowledgements

The authors would like to thank Assoc. Prof. Dr. Viton Uthaisangsuk and Dr. Patcharapit Promoppatum of faculty of engineering, the King Mongkut's University of Technology Thonburi in their advice.



## 7. References

- Ahmad, I., & Al-Harbi, F. (2018). *3D Printing in Dentistry - 2019/2020*.
- Alifui-Segbaya, F., Williams, R., & George, R. (2017). Additive Manufacturing: A Novel Method for Fabricating Cobalt-Chromium Removable Partial Denture Frameworks. *The European journal of prosthodontics and restorative dentistry*, 25, 73-78. doi:10.1922/EJPRD\_1598Alifui-Segbaya06
- ASTM. (2004). ASTM E8-04, Standard Test Methods for Tension Testing of Metallic Materials.
- ASTM. (2013). ASTM F136-13, Standard specification for wrought Titanium-6Aluminium-4Vanadium ELI (extra low interstitial) alloy for surgical implant application.
- Attar, H., Calin, M., Zhang, L. C., Scudino, S., & Eckert, J. (2014). Manufacture by selective laser melting and mechanical behavior of commercially pure titanium. *Materials Science and Engineering: A*, 593, 170-177. doi: 10.1016/j.msea.2013.11.038
- Azarniya, A., Garmendia, X., Mirzaali, M. J., Sovizi, S., Bartolomeu, F., Mare, W., . . . Zadpoor, A. (2019). Additive manufacturing of Ti-6Al-4V parts through laser metal deposition (LMD): Process, microstructure, and mechanical properties. *Journal of Alloys and Compounds*, 804. doi: 10.1016/j.jallcom.2019.04.255
- Choo, H., Sham, K.-L., Bohling, J., Ngo, A., Xiao, X., Ren, Y., & Garlea, E. (2019). Effect of laser power on defect, texture, and microstructure of a laser powder bed fusion processed 316L stainless steel. *Materials & Design*, 164, 107534. doi: 10.1016/j.matdes.2018.12.006
- Dong, S., Zhang, X., Ma, F., Jiang, J., Yang, W., Lin, Z., & Chen, C. (2020). Research on metallurgical bonding of selective laser melted AlSi10Mg alloy. *Materials Research Express*, 7. doi:10.1088/2053-1591/ab6dae
- El-Sayed, M., Ghazy, M., Youssef, Y. M., & Essa, K. (2018). Optimization of SLM process parameters for Ti6Al4V medical implants. *Rapid Prototyping Journal*, 25(3). doi:10.1108/RPJ-05-2018-0112
- Elsayed, M. (2019). Optimization of SLM process parameters for Ti6Al4V medical implants. *Rapid Prototyping Journal*, 25(3), 433-447. doi: 10.1108/RPJ-05-2018-0112
- Frazier, W. E. (2014). Metal Additive Manufacturing: A Review. *Journal of Materials Engineering and Performance*, 23(6), 1917-1928. doi: 10.1007/s11665-014-0958-z
- Gong, H. (2013). *Generation and detection of defects in metallic parts fabricated by selective laser melting and electron beam melting and their effects on mechanical properties*.
- Kusuma, C., Ahmed, S. H., Mian, A., & Srinivasan, R. (2017). Effect of laser power and scan speed on melt pool characteristics of commercially pure titanium (CP-Ti). *Journal of Materials Engineering and Performance*, 26(7), 3560-3568. doi: 10.1007/s11665-017-2768-6
- Liu, J., Song, Y., Chen, C., Wang, X., Li, H., Zhou, C. a., & Sun, J. (2019). Effect of scanning speed on the microstructure and mechanical behavior of 316L stainless steel fabricated by selective laser melting. *Materials and Design*, 108355. doi: 10.1016/j.matdes.2019.108355
- Schulze, C., Weinmann, M., Schweigel, C., Kessler, O., & Bader, R. (2018). Mechanical Properties of a Newly Additive Manufactured Implant Material Based on Ti-42Nb. *Materials (Basel)*, 11(1). doi: 10.3390/ma11010124
- Shipley, H., McDonnell, D., Culleton, M., Coull, R., Lupoi, R., O'Donnell, G., & Trimble, D. (2018). Optimisation of process parameters to address fundamental challenges during selective laser melting of Ti-6Al-4V: A review. *International Journal of Machine Tools and Manufacture*, 128, 1-20. doi: 10.1016/j.ijmachtools.2018.01.003
- Sing, S. L. (2019a). *Selective Laser Melting of Novel Titanium-Tantalum Alloy as Orthopaedic Biomaterial*.
- Sing, S. L. (2019b). *Selective Laser Melting of Novel Titanium-Tantalum Alloy as Orthopaedic Biomaterial. [electronic resource]* (1st ed. 2019. ed.): Springer Singapore.
- Singh, N., Hameed, P., Ummethala, R., Manivasagam, G., Prashanth, K. G., & Eckert, J. (2020). Selective laser manufacturing of Ti-based alloys and composites: impact of process parameters, application trends, and future prospects. *Materials Today Advances*, 8, 100097. doi: 10.1016/j.mtadv.2020.100097



- Song, B., Dong, S., Zhang, B., Liao, H., & Coddet, C. (2012). Effects of processing parameters on microstructure and mechanical property of selective laser melted Ti6Al4V. *Materials & Design*, 35, 120-125. doi: 10.1016/j.matdes.2011.09.051
- Sun, D., Gu, D., Lin, K., Ma, J., Chen, W., Huang, J., & Chu, M. (2019). Selective laser melting of titanium parts: Influence of laser process parameters on macro- and microstructures and tensile property. *Powder Technology*, 342, 371-379. doi: 10.1016/j.powtec.2018.09.090
- Sun, J., Yang, Y., & Wang, D. (2013). Parametric optimization of selective laser melting for forming Ti6Al4V samples by Taguchi method. *Optics & Laser Technology*, 49, 118-124. doi: 10.1016/j.optlastec.2012.12.002
- Trevisan, F., Calignano, F., Aversa, A., Marchese, G., Lombardi, M., Biamino, S., & Manfredi, D. (2017). Additive manufacturing of titanium alloys in the biomedical field: processes, properties and applications. *Journal of Applied Biomaterials & Functional Materials*, 16. doi: 10.5301/jabfm.5000371
- Wang, Z., & Li, P. (2018). Characterisation and constitutive model of tensile properties of selective laser melted Ti-6Al-4V struts for microlattice structures. *Materials Science and Engineering: A*, 725, 350-358. doi: 10.1016/j.msea.2018.04.006
- Wysocki, B., Maj, P., Sitek, R., Buhagiar, J., Kurzydłowski, K. J., & Świączkowski, W. (2017). Laser and Electron Beam Additive Manufacturing Methods of Fabricating Titanium Bone Implants. *Applied Sciences*, 7, 657. doi: 10.3390/app7070657
- Zhang, L.-C., & Attar, H. (2016). Selective Laser Melting of Titanium Alloys and Titanium Matrix Composites for Biomedical Applications: A Review *Advanced Engineering Materials*, 18(4), 463-475. doi: 10.1002/adem.201500419